Excited states in neutron-deficient ^{195}Bi

T. Lönnroth,* C. W. Beausang, D. B. Fossan, L. Hildingsson,†
W. F. Piel, Jr., M. A. Quader, and S. Vajda
Department of Physics, State University of New York, Stony Brook, New York 11794

T. Chapuran
Department of Physics, University of Pennsylvania, Philadelphia, Pennsylvania 19104

E. K. Warburton
Department of Physics, Brookhaven National Laboratory, Upton, New York 11973
(Received 19 December 1985)

Excited states in ^{195}Bi were populated by the ^{182}W(^{19}F,6n) and ^{169}Tm(^{30}Si,4n) reactions. The subsequent γ-ray emission was studied using in-beam spectroscopic methods including excitation functions, γ-ray angular distributions, γ-γ-t coincidence, conversion electron, and pulsed-beam-γ timing measurements. Three isomeric states were located in ^{195}Bi[$J^\pi, t_{1/2}, E$]: [($\frac{13}{2}^+$), 32±2 ns, 888 keV]; [($\frac{25}{2}^+$), 80±10 ns, 2196 keV]; and [($\frac{29}{2}^-$), 750±50 ns, 2311+Δ keV]. The structure of the observed states is interpreted within the shell-model framework. Systematic features of excited state energies and transition rates in the odd-A bismuth isotopes are discussed. A comparison of intruder states analogous to those in odd-A antimony nuclei of the $Z=50$ transition region is made.

I. INTRODUCTION

As is well known, $^{208}_{82}$Pb$_{126}$ is essentially an "inert" spherical nucleus and therefore nuclei with a few valence nucleons outside this core are well suited for testing various properties of the nuclear shell model. For example, detailed calculations have been performed to reproduce the experimental energy spectra of the four(like)-nucleon cases, ^{204}Pb (Ref. 1) and ^{212}Rn (Refs. 2 and 3). Recently, a number of $Z \geq 82$ nuclides with many valence nucleons have been studied in-beam, e.g., ^{204}Rn ($Z=86$, 12 nucleons),[4] ^{201,203}At ($Z=85$, 13, and 11 nucleons) (Ref. 5), and ^{197}Bi ($Z=83$, 13 nucleons).[6] It has been found in these many-nucleon cases that there is still no apparent evidence for deviations from sphericity, and that the properties of the excited yrast states can be interpreted in terms of some few valence nucleons coupled to a spherical core.

When the core is increasingly depleted of neutrons, however, new effects may be expected. First, the large number of neutron holes in the $N=126$ shell may introduce vibrational instability in the Pb core. This effect would then be manifest by a vibrational-type excitation spectrum and by enhanced $E2$ transition rates. In Fig. 1 (lower part) the systematic behavior of the first few yrast excited states in even-A Pb isotopes[7,8] is displayed. As is seen, the lead isotopes do not seem to exhibit yrast vibrational spectra, nor are enhanced $B(E2)$ values found. Second, in the odd-A thallium ($Z=81$) isotopes, $J^\pi = \frac{9}{2}^-$ intruder states appear at relatively low excitation energy. They were interpreted to be one-particle–two-hole (1p-2h) proton states.[9] The analogous 2p-1h excitations are observed in the bismuth isotopes, giving rise to $\frac{1}{2}^+$, $\frac{3}{2}^+$, and $\frac{5}{2}^+$ states,[10] but the $\pi h_{11/2}^{-1}$ intruder has not been observed. Figure 1 (upper part) gives the proton hole sequence as observed in the Tl isotopes. Since the $\frac{11}{2}^-$ intruder states have not been observed in the Bi isotopes, it is an open question whether this proton 2p-1h excitation induces a sufficient lowering of a deformed minimum in the potential energy surface to give rise to observable collective bands, as has been observed in the analogous

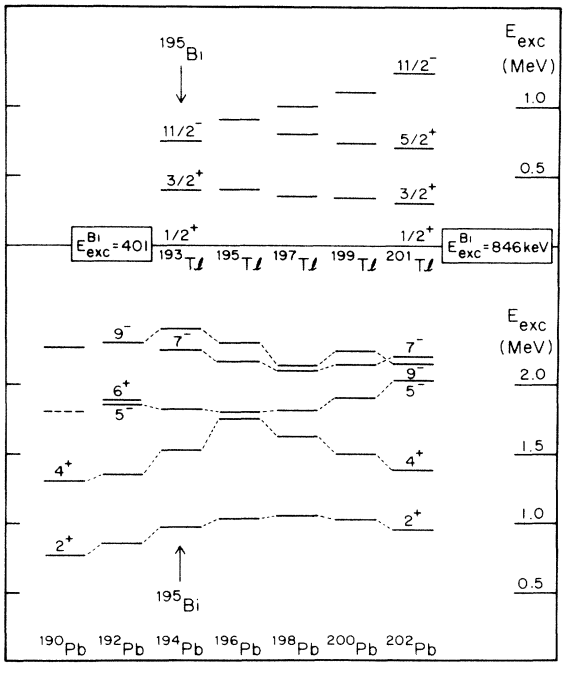

FIG. 1. Systematic behavior of the low-lying 2^+, 4^+, 5^-, 7^-, and 9^- levels in the even-A Pb core nuclei (lower part), and the single-proton hole states in odd-A Tl (upper part), as taken from Refs. 7 and 8. Note the relative energies of Tl, i.e., the $\frac{1}{2}^+$ state is set for reference at zero energy.

$Z=51$ isotopes.[11]

Thus, one of the aims of the present study was to investigate the excited spectrum of ^{195}Bi with an emphasis on the onset of collectivity as outlined above, or conversely, to see how far from the $N=126$ closure the bismuth nuclei maintain sphericity. Moreover, the possibility of finding evidence for the deformed $\pi h_{11/2}^{-1}$ intruder state is greater for ^{195}Bi than for any of the heavier odd-A Bi nuclides studied, since ^{195}Bi is closer to the middle of the neutron shell. In Sec. II the experimental details are presented. The construction of the level scheme is described in Sec. III. In Sec. IV, we discuss the properties of levels in ^{195}Bi and the systematics of the excitation energies and transition rates in the odd-A bismuth isotopes. A discussion of the possibility of shape coexistence and a comparison with the analogous nucleus ^{121}Sb ($Z=51$) is made in Sec. IV D.

II. EXPERIMENTAL PROCEDURE

The excited states in ^{195}Bi were populated in the ^{182}W(^{19}F,6n) and the ^{169}Tm(^{30}Si,4n) reactions using heavy ion beams from both the Brookhaven MP Tandem and the Stony Brook Superconducting LINAC. Since no excited states were known previously, a careful isotopic identification was required. In order to identify transitions belonging to ^{195}Bi, a yield function for ^{19}F+^{182}W was measured over the energy interval $E_{lab}=85-135$ MeV, in steps of 10 MeV. A sputtered 2.4 mg/cm^2 thick tungsten target, enriched to $\sim 80\%$ in ^{182}W, was used; information on the reaction products from the contaminant W isotopes is available. Since levels in ^{197}Bi (4n), ^{196}Pb ($5n\beta^+ + p4n$), and ^{194}Pb ($7n\beta^+ + p6n$) were known,[6,7] a search for γ rays characteristic of the six-particle channel could be made. The upper part of Fig. 2 shows a singles γ-ray spectrum recorded at 115 MeV, and the lower part a delayed ($\Delta t \approx 50-500$ ns) spectrum obtained by pulsing the beam. In Fig. 3 the excitation functions of selected known transitions in ^{197}Bi, ^{196}Pb, and ^{194}Pb, as well as two candidates for ^{195}Bi are shown. As is seen, the curves labeled 888 and 344 keV clearly behave as if they originated from the evaporation of six particles. Unfortunately the reaction-to-background ratio for the neutron-deficient

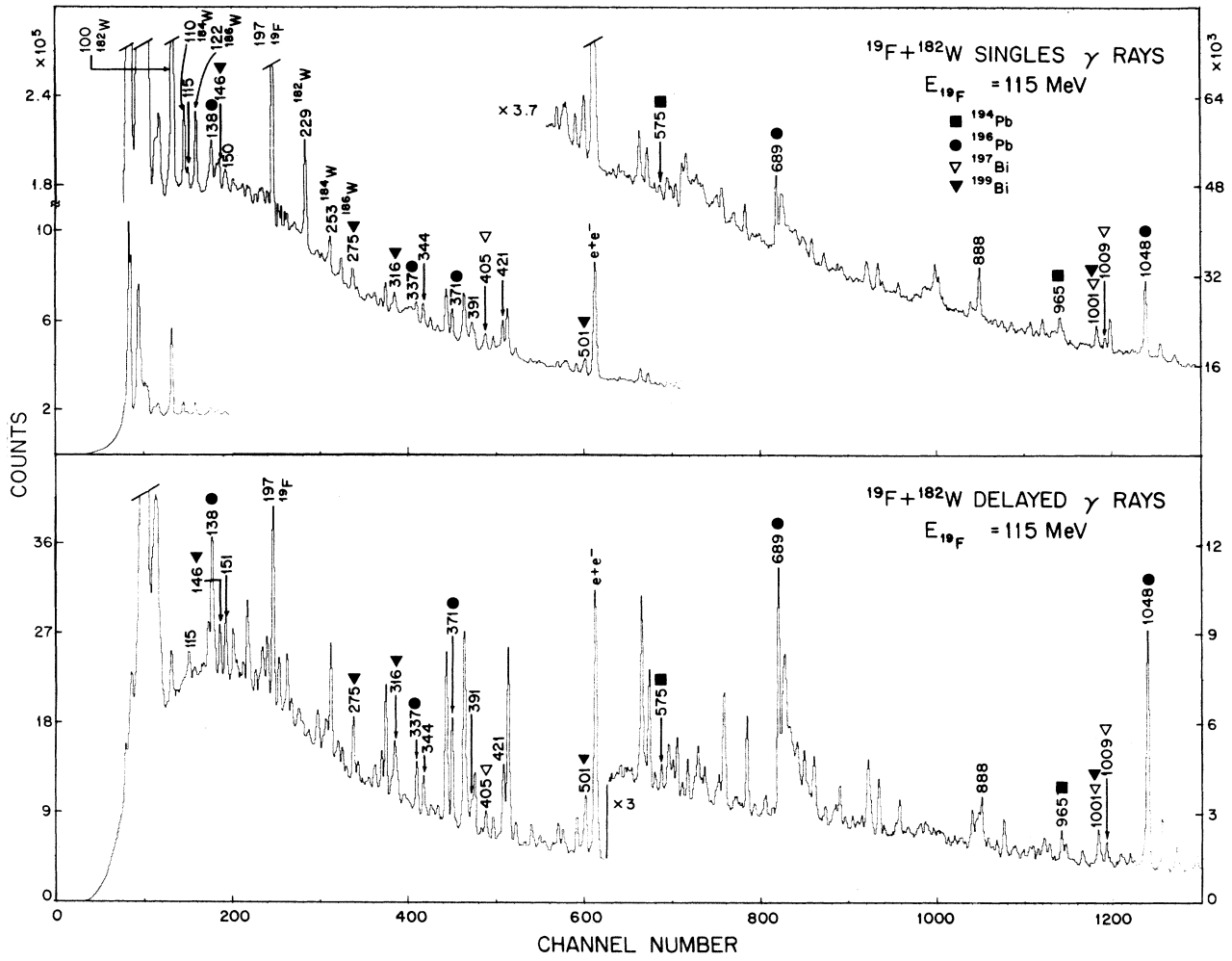

FIG. 2. Singles and delayed ($\Delta t=50-500$ ns) spectra from the reaction ^{19}F+^{182}W at $E_{lab}=115$ MeV. Gamma-ray lines in ^{195}Bi are labeled with their energies in keV. Note the high background (partially from fission products) and the presence of numerous lines from competing reaction channels.

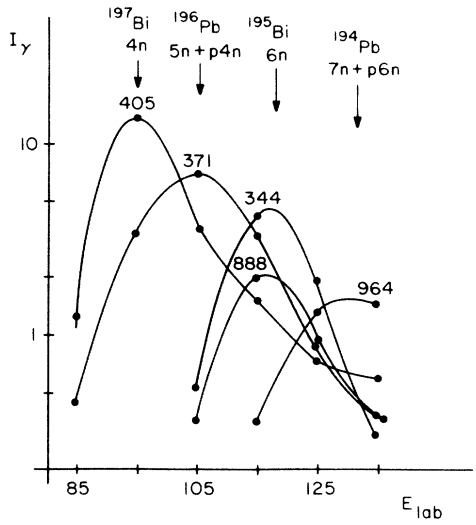

FIG. 3. Excitation functions for transitions assigned in ^{197}Bi (Ref. 6), ^{194,196}Pb (Ref. 7), and two candidates for ^{195}Bi (344 and 888 keV). The relative yields are normalized to the beam current but not corrected for efficiency.

^{195}Bi (6n) channel is not large. Part of the background is believed to originate from fission fragments. On the basis of the excitation functions, the subsequent (^{19}F,6n) measurements were performed with a beam energy of 115 MeV.

The γ-γ-t coincidences were recorded with two large (21% relative efficiency) Ge(Li) detectors placed at $+90°$ and $-110°$ with respect to the beam direction, using the ^{19}F+^{182}W reaction. Figure 4 shows the 888 keV gate for γ rays in a prior (50 ns $< t <$ 500 ns) time window, the 421 keV gate for delayed (50 ns $< t <$ 500 ns) γ rays, and the sum gate, for the entire time range (1 μs), of all transitions assigned to ^{195}Bi. As is seen, all of these spectra show coincidences with bismuth K x rays from converted γ-ray transitions. This fact along with the excitation curves (Fig. 3) allows for unambiguous assignment of these transitions to ^{195}Bi. The pulsed-beam-γ timing measurement was performed to establish isomeric lifetimes. In order to achieve both good time resolution and reasonable intensities, both a small planar and a larger coaxial detector were used. The beam was pulsed with a repetition rate of 1 μs, and a prompt-resolution slope of 7.8 ns at 880 keV was achieved. A delayed spectrum (50 ns $< t <$ 500 ns) is shown in the lower part of Fig. 2. Three background-subtracted time-delay curves are shown in Fig. 5. The 115 and 151 keV curves were obtained with the planar detector and that for the 888 keV γ ray resulted from a coaxial detector. Gamma-ray angular distributions were measured at six angles between 45° and 160° with respect to the beam direction using a detector at 15 cm distance from the target. A second detector at $-90°$ served as a

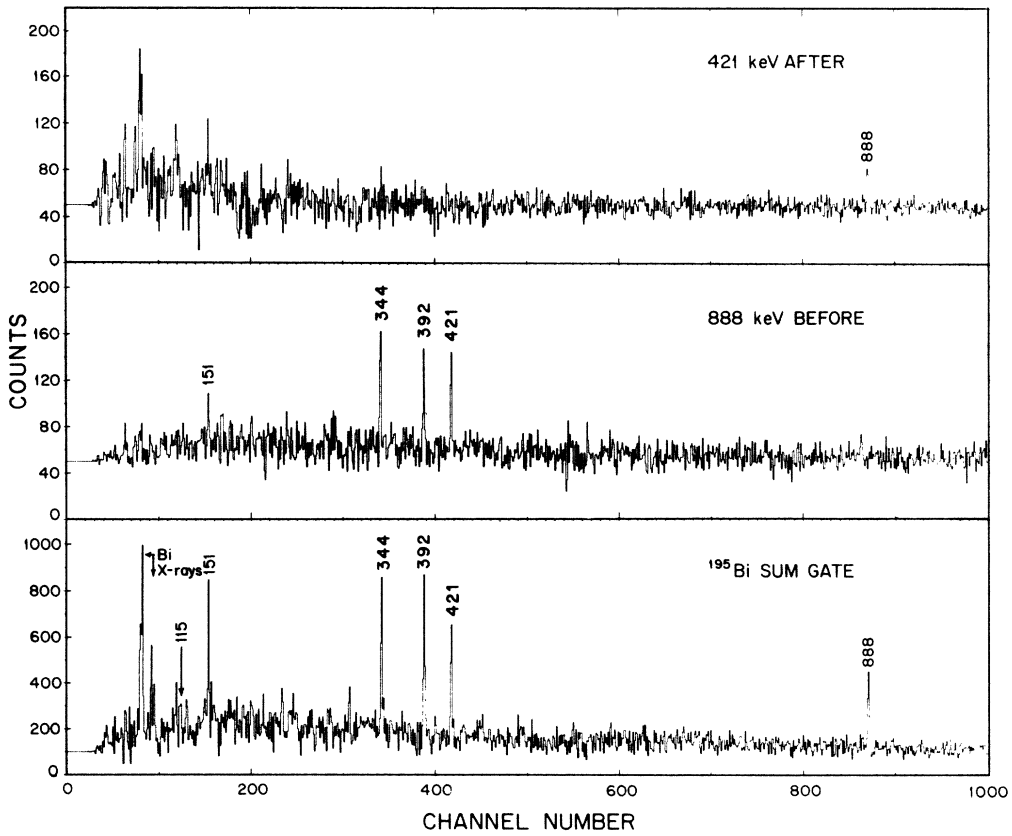

FIG. 4. Sample background-subtracted γ-γ coincidence spectra including the presence of coincident Bi x rays (see discussion in the text).

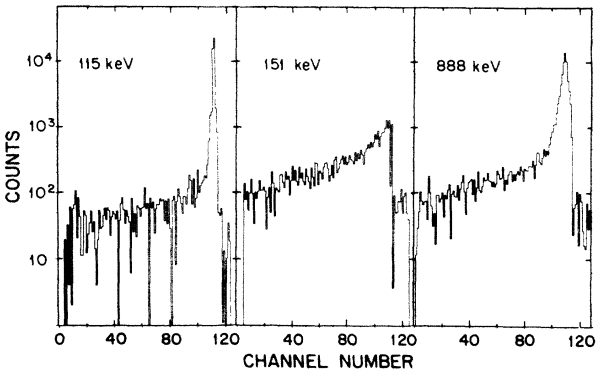

FIG. 5. Time-delay curves for three transitions assigned to ^{195}Bi. The 115 and 151 keV curves were obtained from the planar detector and the 888 keV curve from the coaxial detector. The 115 keV decay curve contains only the 0.75 μs half-life components plus a prompt part, the 151 keV curve contains both the 0.75 μs and 80 ns components with no prompt contributions, and the 888 keV curve has both of these components plus a 32 ns half-life component.

monitor. The normalized γ-ray intensities were fitted to the Legendre polynomial

$$W(\theta)=I_\gamma[1+A_{22}P_2(\cos\theta)+A_{44}P_4(\cos\theta)]\ ,$$

from which the angular-distribution coefficients $A_{22}=A_2/A_0$ and $A_{44}=A_4/A_0$ were obtained. The properties of the ^{195}Bi γ rays extracted from angular-distribution and timing measurements are collected in Table I.

A mini-orange electron spectrometer,[12] recently fabricated at Stony Brook, was used to record the conversion electrons produced (at $\theta=125°$) by the ^{169}Tm(^{30}Si,4n)^{195}Bi reaction at 142 MeV. The ^{169}Tm target was 800 μg/cm^2 on either a kapton backing (1.9 mg/cm^2) or a lead backing (3.8 mg/cm^2). The beam was stopped several meters downstream, while the backing served to stop the reaction products. In order to minimize the background from delta rays, only electrons detected between the beam pulses

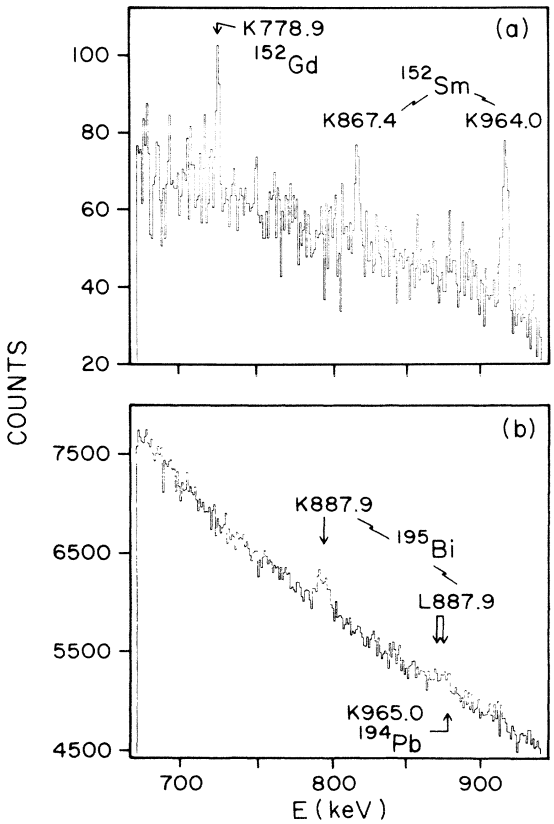

FIG. 6. (a) Energy calibration for part of the conversion electron spectrum using a ^{152}Eu source at the target position. (b) Delayed conversion electron spectrum near 800 keV taken in-beam for ^{169}Tm + ^{30}Si (see discussion in the text).

(106 ns repetition period) were recorded. The energy calibration of the Si(Li) detector was obtained by replacing the target with an ^{152}Eu source for about 30 min. Part of the ^{152}Eu spectrum around 800 keV is shown in Fig. 6(a) while the corresponding part of the in-beam spectrum is shown in Fig. 6(b). The K- and L-conversion peaks of the

TABLE I. Properties of transitions assigned to ^{195}Bi from the ^{19}F + ^{182}W data.

E (keV)	I_γ^a	I_{tot}^b	A_2/A_0	A_4/A_0	$T_{1/2}$ (ns)[c]	Multipolarity[d]
115.2	5(3)	35(20)			750(100)	($M1$)
151.3	20(4)	46(10)	~0		770(100),90(20)	($E2$)
344.3	84(6)	85(6)	−0.20(17)	+0.2(2)	800(100),70(20)	Dipole
391.7	67(6)	68(6)	−0.25(7)	+0.03(9)	730(80),85(20)	Dipole
421.0	62(6)	64(6)	+0.42(6)	−0.46(9)	720(80),75(20)	($E2$)
887.9	100	100	+0.09(7)	+0.02(10)	800(120),70(30) 32(2)	$M2(+E3)$

[a]Normalized to the 887.9 keV transition. The gamma-ray intensities of the 115.2 and 151.3 keV transitions are estimated from the coincidence spectra.

[b]Intensity corrected for the conversion (Ref. 13) of the adopted multipolarities.

[c]From multiple lifetime fits to the time-delay curves for the respective photopeaks. Weighted means give as final results: $t_{1/2}=32(2)$ ns, 80(10) ns, and 750(50) ns for the 888, 2196, and (2311 + Δ) keV levels, respectively.

[d]For parity arguments, including conversion electron results, see the text.

888 keV ground-state transition can be seen. The experimental result for α_K is 0.082±0.015, while the calculated value[13] for $M2$ is 0.0543 and for $E3$ is 0.0155. The 888 keV transition thus appears to be either an $M2$ or an $M2/E3$ admixture, since the experimental result is within two standard deviations above the calculated $M2$ value and the possibility of $M3$ or higher multipolarities can be ruled out by lifetime considerations.

Since the 344 and 392 keV transitions are dipole in nature from the angular distributions, it was hoped that the electron conversion measurements could determine their $M1$ or $E1$ character since the $M1$ conversion coefficient is approximately a factor of 10 larger than that for an $E1$. Unfortunately, the background resulting from the γ decay of the fission fragments made it difficult to extract the conversion electron peaks in this energy region. In both cases, the electron yields did not allow one to rule out the $M1$ possibility; although the experimental upper limit for the 344 keV K electrons was about half the calculated $M1$ value, an $M1/E2$ admixture with significant $E2$ mixing is still possible. Thus, the magnetic or electric character of these dipoles is not defined. No conversion electron information could be extracted from the remaining ^{195}Bi transitions.

Finally, the ^{169}Tm(^{28}Si,4n) reaction was used in a search for excited states in ^{193}Bi, where the $\frac{13}{2}^+$ state was predicted at an excitation energy of 460±50 keV (see Sec. IV C), and to have a half-life of about 0.5 μs. Despite the analogy to the ^{169}Tm(^{30}Si,4n) reaction which was used to populate excited states in ^{195}Bi, no transitions were found which could be assigned to ^{193}Bi. This is probably due to two effects. First, the fission cross section increases in neutron deficient isotopes and second, the probability of charged-particle emission increases rapidly in the vicinity of the proton drip line.

III. LEVEL SCHEME OF ^{195}Bi

The level scheme of ^{195}Bi obtained from the present work is displayed in Fig. 7. The proposed J^π assignments, which are tentative, are based on angular distributions, lifetime information, conversion electron results, and systematic properties of the odd-A Bi isotopes. As mentioned in Sec. II, the transitions were assigned to this nuclide on the basis of the excitation functions and the Bi x-ray coincidences. We assume that the cascade obtained from the γ-γ coincidence data ultimately feeds the presumed $\frac{9}{2}^-$ ground state ($\pi h_{9/2}$) as in the heavier odd-A Bi isotopes. In ^{195}Bi two low-lying states are anticipated, namely the odd 83rd proton $\frac{9}{2}^-$ state and the intruder $\frac{1}{2}^+$ state (cf. Refs. 7 and 10), but since the nucleus is produced in a (HI,xn) reaction, the former will be predominantly populated. The 888 keV transition is placed as feeding the ground state, for which $J^\pi=(\frac{9}{2}^-)$ is assumed, since it has the largest intensity and it is seen in the delayed region for all the other γ-ray gates in the cascade. Moreover, the 888 keV γ ray is the only one showing the $t_{1/2}=32$ ns time component (Fig. 5). A spin and parity of $(\frac{13}{2}^+)$ are assigned to the $t_{1/2}=32$ ns level since the 888 keV transition is of $M2(+E3)$ multipolarity as discussed above. The next transitions in the cascade based on intensity and prompt time components, are γ rays of 344, 392, and 421 keV. Since the first two are $E1$ or $M1$ dipoles and the third of $E2$ character (Table I), they define for stretched transitions the level spins ($\frac{15}{2}$, 1232 keV), ($\frac{17}{2}$, 1624 keV), and ($\frac{21}{2}$, 2045 keV), with the adoption of $(\frac{13}{2}^+)$ for the 888-keV excited state. The ordering of the two topmost transitions shown in Fig. 7, 151 and 115 keV, is made on the basis of their time-delay curves (Fig. 5), from which it is concluded that the 115 keV γ ray shows the 0.75 μs half-life only, and the 151 keV transition depopulates a $t_{1/2}\sim 80$ ns isomeric state. Since the 115 keV γ ray has a prompt component, the most probable multipolarity is $M1$, and the 80 ns half-life of the 151 keV transition is compatible with $E2$ multipolarity. From the systematic behavior of the heavier Bi isotopes, the 151 keV transition is assigned to be the expected $\frac{25}{2}^+ \rightarrow \frac{21}{2}^+$ transition. These arguments give spin parities of ($\frac{21}{2}^+$, 2045 keV), ($\frac{25}{2}^+$, 2196 keV), and ($\frac{27}{2}^+$, 2311 keV). With these assignments, the 344 and 392 keV stretched dipoles have to be either both $E1$ or both $M1$ transitions. The $E1$ choice proposed, which implies the ($\frac{15}{2}^-$, 1232 keV) assignment, is based on systematics (see discussion below) and a slight preference for a 344-keV $E1$ by the conversion electron measurements. Finally, since a half-life of about 0.75 μs is seen in all of the time curves, the existence of an isomeric state above 2311 keV is inferred, although no low-energy γ ray is seen. An estimate for the energy of the unobserved transition and thus the energy of this isomer is made in Sec. IV B. On the basis of the systematic behavior in heavier odd-A Bi nuclides, the isomer probably is the expected $\frac{29}{2}^-$ level.

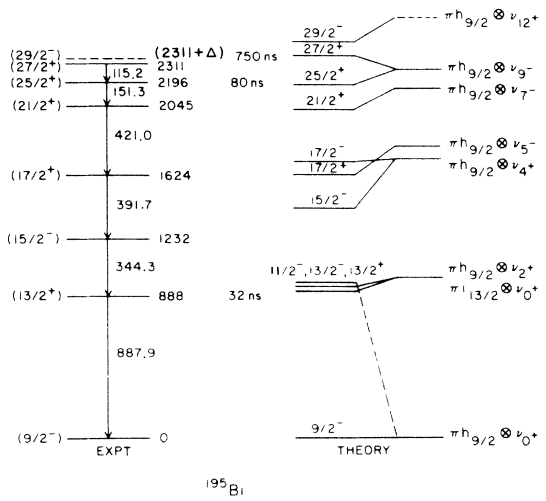

FIG. 7. Level scheme of ^{195}Bi as obtained in the present work. The calculated levels and configurations are given to the right, cf. Sec. IV for details.

IV. DISCUSSION

A. Excitation energies and configurations in ^{195}Bi

In the recent studies of ^{201,199,197}Bi, a method of calculating the energies of three-quasiparticle states in the light odd-A bismuth isotopes was presented.[6,14] The tests made in those nuclei showed that energies could be predicted

with an accuracy of about 100 keV or better. The same method was applied to ^{195}Bi given the levels and configurations on the right-hand side of Fig. 7. The 888 keV state is most probably due to the $i_{13/2}$ proton because of the $t_{1/2}=32$ ns isomerism. The $\frac{13}{2}^+$ state drops nonlinearly if compared to the heavier Bi isotopes. This is expected since the $i_{13/2}$ proton has the smallest repulsion with respect to the increasing population of $\nu i_{13/2}$ holes.[15]

The $\frac{11}{2}^-$ and $\frac{13}{2}^-$ states of the $\pi h_{9/2}\otimes\nu 2^+$ configuration are expected to be nearly degenerate with the $\pi i_{13/2}\otimes\nu 0^+$ state in ^{195}Bi. Experimentally this is the first isotope where the $\frac{13}{2}^+$ state is lower in energy than the other two. For the $(\frac{15}{2}^-)$ state at 1232 keV, the only plausible configurations is $\pi h_{9/2}\otimes\nu 4^+$. Note that positive parity can be obtained only from the $\pi h_{9/2}\otimes\nu 5^-$ or $\pi i_{13/2}\otimes\nu 2^+$ configurations, both of which are estimated to occur at about 1700 keV. The energy deviation with theory for the $\frac{15}{2}^-$ state might be due to the presence of two admixed 4^+ states. The calculated energy for the $\frac{17}{2}^+$ state of the $\pi h_{9/2}\otimes\nu 5^-$ configuration comes very close to the experimental $(\frac{17}{2}^+)$ state at 1624 keV, supporting this configuration assignment. For the next three levels the configurations $\pi h_{9/2}\otimes\nu 7^-$, $J^\pi=\frac{21}{2}^+$ and $\pi h_{9/2}\otimes\nu 9^-$, $J^\pi=\frac{25}{2}^+$, $\frac{27}{2}^+$ are consistent with the experimental findings. Because the systematics of the heavier isotopes show two $\frac{27}{2}^+$ states at these energies, the contributions of the $\pi h_{9/2}\otimes\nu 9^-$ configuration to these states are not definite. Finally, the $\frac{29}{2}^-$ state of the $\pi h_{9/2}\otimes\nu 12^+$ configuration is expected at about 2400 keV, and it should decay with an $E1$ hindrance of about 10^6 to the $\frac{27}{2}^+$ state. A competing $M2$ transition to the $\frac{25}{2}^+$ state is expected to be very strongly hindered because it has to proceed effectively as

$$\nu(i_{13/2}^{-2})10^+\rightarrow\nu(i_{13/2}^{-1}h_{9/2}^{-1})9^-$$

and these components should have fairly small amplitudes in the $\frac{29}{2}^-$ and $\frac{25}{2}^+$ states. The 0.75 μs isomer is thus a very good candidate for the above-mentioned $\frac{29}{2}^-$ state.

If the identification of the six experimentally observed states is correct, the mean and rms deviations between experiment and calculation are -61 and 85 keV, which can be considered satisfactory in view of the simplifications made in the calculations. We also note that there is no increase in these deviations as compared to the heavier isotopes $^{201-197}$Bi, cf. Refs. 6 and 14. In what follows, the proposed J^π assignments will be assumed.

B. Isomeric transition rates

In ^{195}Bi three isomers at 888, 2196, and 2311 + Δ keV were found involving the $\frac{13}{2}^+\rightarrow\frac{9}{2}^-$, $\frac{25}{2}^+\rightarrow\frac{21}{2}^+$, and $\frac{29}{2}^-\rightarrow\frac{27}{2}^+$ transitions. The half-life of the 888 keV $\frac{13}{2}^+\rightarrow\frac{9}{2}^-$ $M2$ transition corresponds to a hindrance of about 20 over the Weisskopf estimate, and this hindrance is probably due to its spin-flip character. The near-isotropy of this transition can be explained by an $E3$ admixture ($-16\leq\delta\leq-0.15$), expected by extrapolation from the $B(E3)$ values for the $\pi h_{9/2}\rightarrow\pi i_{13/2}$ transitions in ^{210}Po (Ref. 16) and ^{209}Bi (Ref. 17). The $\frac{25}{2}^+\rightarrow\frac{21}{2}^+$ $E2$ transition has a half-life corresponding to about 0.6 W.u. This is a clear indication that collective components in the wave functions are small for these two states in ^{195}Bi, and that the states can be interpreted as being of a quasiparticle nature. The half-life of the assumed $(\frac{29}{2}^-\rightarrow\frac{27}{2}^+)$ transition can be used to estimate the excitation energy of the $t_{1/2}=0.75$ μs isomeric state (see Fig. 6). The half-life of the unobserved $E1$ transition is proportional to the factor $[(1+\alpha_{\rm tot})E_\gamma^3]^{-1}$. Since this factor is slowly varying for E_γ between the atomic shell energies,[13] it can be used to estimate the $E1$ half-lives (where the empirical 10^6 hindrance for this region is included). For $E_\gamma=32$–84 keV one obtains $t_{1/2}=0.6(4)$ μs, for $E_\gamma=18$–32 keV one has $t_{1/2}=2.6(8)$ μs, and for the next intervals much longer. Hence the first energy interval corresponds to a hindrance of $1.3(9)\times10^6$, which is the most plausible. This interval along with the experimental constraint (Sec. III) yields $E_\gamma=41\pm9$ keV and suggests the location of the $\frac{29}{2}^-$ level at $E\sim2350$ keV, under these assumptions.

C. Systematic behavior of yrast states

The comparison of the yrast states in the odd-A Bi isotopes (see Figs. 7 and 8), shows the main cascades to proceed via the following states: $\frac{9}{2}^-$ (g.s., $\pi h_{9/2}\otimes\nu 0^+$); $\frac{11}{2}^-$, $\frac{13}{2}^-$ ($\pi h_{9/2}\otimes\nu 2^+$); $\frac{13}{2}^+$ ($\pi_{13/2}\otimes\nu 0^+$); $\frac{15}{2}^-$, $\frac{17}{2}^-$ ($\pi h_{9/2}\otimes\nu 4^+$); $\frac{17}{2}^+$ ($\pi h_{9/2}\otimes\nu 5^-$); $\frac{21}{2}^+$ ($\pi h_{9/2}\otimes\nu 7^-$); $\frac{25}{2}^+$, $\frac{27}{2}^+$ ($\pi h_{9/2}\otimes\nu 9^-$); $\frac{29}{2}^-$, $\frac{31}{2}^-$ ($\pi h_{9/2}\otimes\nu 12^+$); $\frac{33}{2}^-$, $\frac{35}{2}^-$, and $\frac{37}{2}^-$ ($\pi h_{9/2}\otimes\nu 14^+,16^+$). The ordering and the spacing of these levels depend sensitively on the corresponding neutron states in the even Pb core nuclei. One feature in the light Bi isotopes is that the $\frac{13}{2}^+$ states drop in energy as the neutron number N decreases. This state is interpreted as the $\pi i_{13/2}$ proton state, and its decreasing excitation energy can be understood from the $\pi\nu^{-1}$ two-nucleon interaction energies. With increasing hole population in the $\nu i_{13/2}$ orbital, the $\pi i_{13/2}$ state appears depressed vs the $\pi h_{9/2}$ ground state since the $\pi i_{13/2}\nu i_{13/2}$ multiplet has the smallest repulsion.[18] This behavior was used to predict the excitation energy of the $\frac{13}{2}^+$ state in ^{193}Bi. One obtains 460 keV with an uncertainty of about 50 keV. This transition energy would correspond to a half-life of about 0.5 μs.

As mentioned above, ^{195}Bi seems to be the first nucleus where the $\pi i_{13/2}$ proton state is below the $\pi h_{9/2}\otimes\nu 2^+$ $J^\pi=\frac{11}{2}^-$, $\frac{13}{2}^-$ doublet that is related to the 965-keV 2^+ state in ^{194}Pb. The trend of approximately constant energy observed in the heavier isotopes for the $\frac{17}{2}^+$ state continues. The same effect is observed for the $\frac{25}{2}^+$ state. The reduced splitting of the $\frac{25}{2}^+$-$\frac{27}{2}^+$ states, cf. Fig. 8, might be due to an increased admixture of the $\nu f_{7/2}$ and $\nu h_{9/2}$ orbitals in the 9^- core state, which is thought to be mainly $\nu i_{13/2}^{-1}\nu f_{5/2}^{-1}$. This admixture then reduces the repulsion of the $\frac{27}{2}^+$ state and tends to bring the $J_{\rm max}$ and $J_{\rm max}-1$ states closer.

We also want to stress the seemingly unusual behavior of the $\frac{15}{2}^-$ state, which is interpreted to arise from the $\pi h_{9/2}\otimes\nu 4^+$ configuration. This state is present between the $\frac{13}{2}^-$ and $\frac{13}{2}^+$ states in $^{207-201}$Bi, it is missing in ^{199,197}Bi, and then back almost at its original energy in

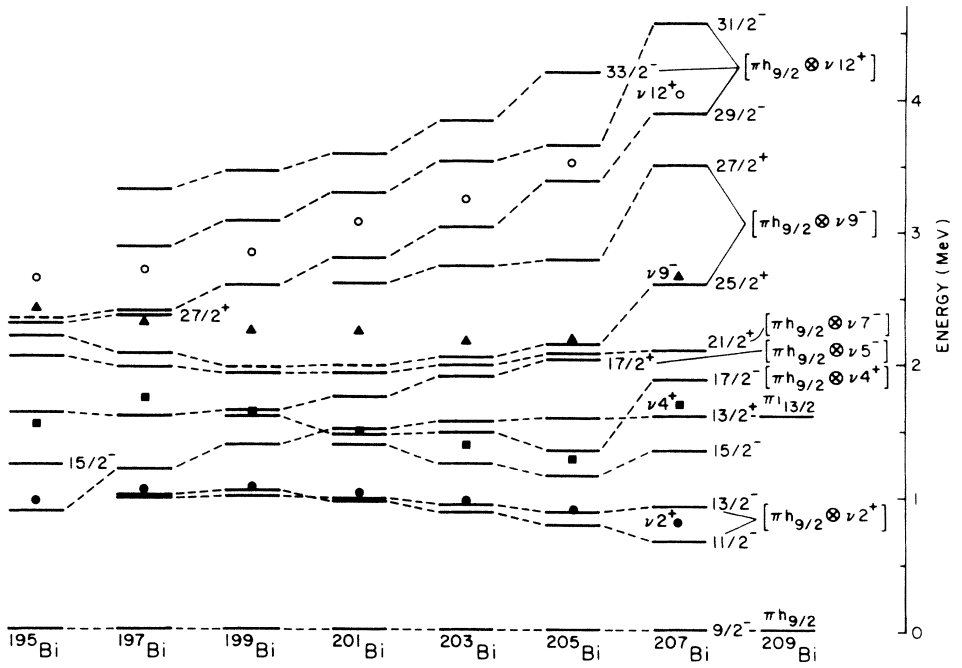

FIG. 8. Systematics of low-lying yrast states of odd-A bismuth isotopes. The results for ^{195}Bi are from the present work, and those for the heavier isotopes are from Refs. 6, 14, 21, and 22.

^{195}Bi. This irregular behavior can be traced to the relative positions of the 4^+ and 5^- core states. As can be seen in Fig. 1 these two states are rather well separated in the heavier Pb isotopes, they become almost degenerate in ^{196}Pb and then separate again in the lighter ones. This feature then provides an explanation for the nonyrast behavior of the $\pi h_{9/2} \otimes \nu 4^+$ $J^\pi = \frac{15}{2}^-$ states in ^{197,199}Bi that are related to the ^{196,198}Pb cores.

D. Particle-hole intruder states, and a comparison of $Z = 82 + 1$ ^{195}Bi with $Z = 50 + 1$ ^{121}Sb

Since both $Z = 50$ and $Z = 82$ are observed to be good proton shell closures, it is of interest to compare the excited spectra of analogous single odd-proton nuclei of both regions, e.g., Bi ($Z = 83$) and Tl ($Z = 81$) for the lead region and Sb ($Z = 51$) and In ($Z = 49$) for the tin region. Thus in the present work the lead-region nuclides ^{195}Bi-^{193}Tl are compared to ^{121}Sb-^{119}In of the tin region, as shown in Fig. 9. The structures of the four nuclei of these two regions are rather similar, as could be expected, although there are some interesting differences. First, the proton gaps across the $Z = 50$ or 82 closures are both fairly large, but their magnitudes are different, about 3 MeV in ^{194}Pb and 4.9 MeV in ^{120}Sn. Second, the 2^+ and 4^+ excitation energies are rather similar, 965 and 1539 keV in ^{194}Pb and 1172 and 2195 keV in ^{120}Sn. But the odd-proton nuclei behave in different ways. The $Z = 49$ nucleus ^{119}In shows most of the single proton-hole orbitals of the $Z = 28$–50 shell ($f_{5/2}$, $p_{3/2}$, $p_{1/2}$, and $g_{9/2}$), whereas the $Z = 81$ nucleus ^{193}Tl shows, at energies comparable to those of ^{119}In, only the first two proton-hole orbitals $s_{1/2}$ and $d_{3/2}$. In ^{193}Tl an "intruder" $\frac{9}{2}^-$ state, interpreted to be the $\pi j^{-2} 0^+ \pi h_{9/2}$ proton core excitation,[9] appears already at about 400 keV. This state, with a $[505]\frac{9}{2}^-$ Nilsson configuration, then has a $\Delta J = 1$ band

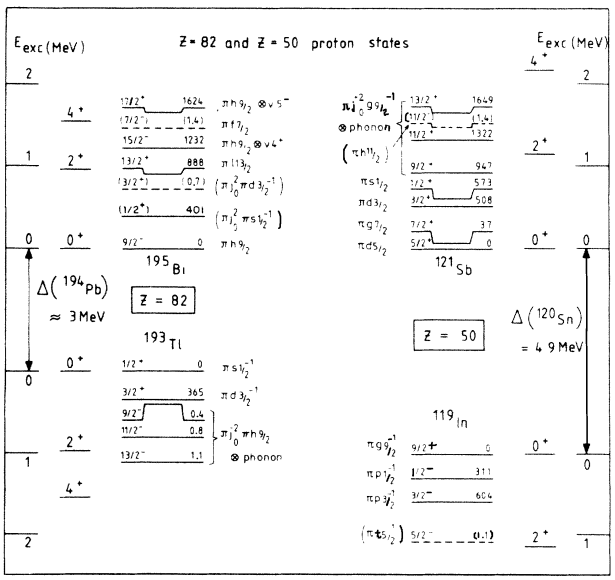

FIG. 9. Comparison of the excited structures of ^{195}Bi-^{193}Tl at $Z = 82$ to the analogous ^{121}Sb-^{119}In pair in $Z = 50$. All four level schemes are drawn to the same energy scale, whereas the gaps are not. Dashed levels with spin parity and energy in parentheses are an estimate extrapolated from the neighboring isotopes.

built upon it. In contrast to these proton-hole nuclides, the proton-particle nucleus ^{121}Sb shows all five proton orbitals of the $Z=50-82$ shell ($s_{1/2}$, $d_{3/2}$, $d_{5/2}$, $g_{7/2}$, and $h_{11/2}$), and in addition, the intruder $\pi g_{9/2}^{-1}$ state $[404]\frac{9}{2}^+$ with a deformed $\Delta J=1$ band, as in ^{193}Tl. From this one would expect that the $[505]\frac{11}{2}^-$ bandhead, the $\pi j^2 0^+ \pi h_{11/2}^{-1}$ proton core excitation, should appear in ^{195}Bi at a relatively low excitation energy, since the low-spin particle-hole excitations involving the $s_{1/2}$ and $d_{3/2}$ orbitals can be rather accurately determined. The $s_{1/2}$ state is located at 401 keV in ^{195}Bi as found in recent α-decay work.[19] However, the $\frac{11}{2}^-$ intruder state is not observed. As was pointed out,[9] there should be a substantial gain in energy from a particle-hole excitation, as has been verified in Tl and Sb. However, if the core is deformed to the oblate minimum, the $\Omega^\pi=\frac{11}{2}^-$ intrinsic state would acquire an additional repulsion, and this might be the explanation of the nonobservation of the $[505]\frac{11}{2}^-$ band in ^{195}Bi. Indeed, in ^{193}Tl the observed $\Delta J=1$ band is typical for a strongly coupled band on an oblate core, whereas the $\pi g_{9/2}$ hole in the Sb isotopes appears coupled to a prolate core. It is of interest to point out that the intruder states seem to induce oblate deformation of the Pb cores. In a recent work[20] on light even Pb isotopes, it was found that in $^{192-198}$Pb low-lying 0^+ states occur. The calculation presented there indicated that these states are of the 2p-2h proton configurations $\{\frac{1}{2}^+[440]^{-2}\,\frac{9}{2}^-[514]^2\}\Omega=0$, and that this configuration attains a minimum energy in ^{196}Pb for a quadrupole deformation $\epsilon_2=-0.1$. Another effect which may affect the observation of the intruder $\frac{11}{2}^-$ state is the fact that the proton $\pi i_{13/2}$ orbital comes low in energy, and thus being an yrast state, it might preclude the observation of the nonyrast $\pi h_{11/2}^{-1}$ state.

The work was supported in part by the National Science Foundation and the Department of Energy.

*On leave from Physics Department, University of Jyväskylä, 40100 Jyväskylä, Finland.

†Permanent address: Research Institute of Physics, Stockholm, Sweden.

[1]C. G. Linden, I. Bergström, J. Blomqvist, and C. Roulet, Z. Phys. A **284**, 217 (1978).

[2]D. Horn, O. Häusser, B. Hass, T. K. Alexander, T. Faestermann, H. R. Andrews, and D. Ward, Nucl. Phys. **A317**, 529 (1979).

[3]T. Lönnroth, J. Phys. (Paris) Lett. **41**, L185 (1980).

[4]D. Horn, C. Baktash, and C. J. Lister, Phys. Rev. C **24**, 2136 (1981).

[5]K. Dybdal, T. Chapuran, D. B. Fossan, W. F. Piel, Jr., D. Horn, and E. K. Warburton, Phys. Rev. C **28**, 1171 (1983).

[6]T. Chapuran, K. Dybdal, D. B. Fossan, T. Lönnroth, W. F. Piel, Jr., D. Horn, and E. K. Warburton, Phys. Rev. C **33**, 130 (1986).

[7]*Table of Isotopes,* 7th ed., edited by C. M. Lederer and V. S. Shirley (Wiley, New York, 1978).

[8]C. Roulet, G. Albouy, G. Auger, J. M. Lagrange, M. Pautrat, K. G. Rensfelt, H. Richel, H. Sergolle, and J. Vanhorenbeeck, Nucl. Phys. **A285**, 156 (1977).

[9]J. Blomqvist, SUNY at Stony Brook Nuclear Theory Group Progress Report, 1969 (unpublished), p. 29.

[10]R. A. Braga, W. R. Western, J. L. Wood, R. W. Fink, R. Stone, C. R. Bingham, and L. L. Riedinger, Nucl. Phys. **A349**, 61 (1980).

[11]R. E. Shroy, A. K. Gaigalas, G. Schatz, and D. B. Fossan, Phys. Rev. C **19**, 1324 (1979).

[12]J. Van Klinken and K. Wisshak, Nucl. Instrum. Methods **98**, 1 (1972).

[13]R. Rösel, H. M. Fries, K. Alder, and H. C. Pauli, At. Data Nucl. Data Tables **21**, 291 (1978).

[14]W. F. Piel, Jr., T. Chapuran, K. Dybdal, D. B. Fossan, T. Lönnroth, D. Horn, and E. K. Warburton, Phys. Rev. C **31**, 2087 (1985).

[15]R. D. Lawson, *Theory of the Nuclear Shell Model* (Clarendon, Oxford, 1980), p. 349.

[16]B. Fant, Phys. Scr. **4**, 175 (1972).

[17]J. W. Hertel, D. G. Fleming, J. P. Schiffer, and H. E. Gove, Phys. Rev. Lett. **23**, 488 (1969).

[18]T. Lönnroth, University of Jyväskylä, Research Report No. 4/81, 1981.

[19]E. Coenen, K. Deneffe, M. Huyse, P. Van Duppen, and J. L. Wood, Phys. Rev. Lett. **54**, 1783 (1985).

[20]P. Van Duppen, E. Coenen, K. Deneffe, M. Huyse, K. Heyde, and P. Van Isacker, Phys. Rev. Lett. **52**, 1974 (1984).

[21]H. Hübel, M. Guttormsen, K. P. Blume, J. Recht, A. von Grumbkow, K. Hardt, P. Schüler, Y. K. Agarwal, and A. Maj, Z. Phys. A **314**, 89 (1983).

[22]T. Lönnroth, J. Blomqvist, I. Bergström, and B. Fant, Phys. Scr. **19**, 233 (1979).